



## Development of a field deployable handheld electrochemical biosensor for detection of aflatoxin B1 in grains

David Mtweve<sup>\*1</sup>, Neema Kassim<sup>2</sup>, Ally Mahadhy<sup>3</sup>

<sup>1</sup>*Department of Health and Biomedical Sciences (HBS), Nelson Mandela African Institution of Science and Technology, Arusha, Tanzania*

<sup>2</sup>*Department of Food Biotechnology and Nutritional Sciences, Nelson Mandela African Institution of Science and Technology, Arusha, Tanzania*

<sup>3</sup>*Department of Molecular Biology and Biotechnology, University of Dar es Salaam, Dar es Salaam, Tanzania*

**Key words:** Aflatoxins, Electrochemical biosensor, Aflatoxin B1, Screen-printed electrode,

Differential pulse voltammetry, Limit of detection

<http://dx.doi.org/10.12692/ijb/25.1.242-254>

Article published on July 10, 2024

### Abstract

Aflatoxins (AFs) are highly toxic, with Aflatoxin B1 (AFB1) being the most harmful, necessitating quick on-site detection to ensure food safety. This study introduces a portable electrochemical biosensor for detecting AFB1 in grains. The biosensor uses a screen-printed electrode (SPE) pretreated in sulfuric acid and modified with bovine serum albumin (BSA) to attach antibodies to the BSA-terminal carboxylic groups, preventing nonspecific AFB1 binding. Modified SPEs were rinsed and stored at 4°C. AFB1 detection was performed using Differential Pulse Voltammetry (DPV) with a wireless portable potentiostat. Absence or low concentrations of AFB1 resulted in a significant increase in DPV peak current, indicating reduced binding of AFB1 to the SPE. Conversely, the presence of AFB1 decreased the DPV peak current, signifying binding of AFB1 to the anti-AFB1 antibodies on the SPE. The signal was transmitted to a cellphone via Bluetooth. The biosensor exhibited a low limit of blank sample (LoB) at 1.67 ng/mL, a low Limit of Detection (LoD) at 2.058 ng/mL, and a dynamic range of 1-20 ng/mL. It was successfully tested on real samples, detecting AFB1 in peanuts and maize flour, indicating its potential for on-site mycotoxin monitoring in food.

\* **Corresponding Author:** David Mtweve ✉ [mtwevedavid@gmail.com](mailto:mtwevedavid@gmail.com)

## Introduction

Mycotoxins are low molecular weight toxic substances produced naturally by fungi as secondary metabolites. These fungi are capable of proliferating on a range of food and feed crops, including cereals, spices and nuts, when specific temperature and humidity conditions are met (Pickova *et al.*, 2020). The most commonly observed mycotoxins of concern to livestock and human health include aflatoxins, ochratoxin A, fumonisin, zearalenone, patulin, and deoxynivalenol/nivalenol. These mycotoxins are harmful to both human and animal where they can cause acute and chronic toxicity, carcinogenicity, mutagenicity, and immunosuppression. Aflatoxins are the most potent and prevalent type of mycotoxins (Kassim *et al.*, 2023; Magoha *et al.*, 2014; Mollay *et al.*, 2020; Mollay *et al.*, 2022; Phillips *et al.*, 2020; Pickova *et al.*, 2020), produced by *Aspergillus* species. Fumonisin is a mycotoxin produced by *Fusarium proliferatum*, *Fusarium verticillioides* and other *Fusarium* spp. *Fusarium* mainly contaminates corn, corn-related products, wheat, and rice and their associated products, while posing a health risk and toxicity to human and animals such as immunotoxicity, acute toxicity, reproductive toxicity, and organ toxicity on humans and animals (Chen *et al.*, 2021; Kamle *et al.*, 2019; Phillips *et al.*, 2020; Smith, 2018; Smith, 2007; Steyn, 2023). Aflatoxin contamination in cereal and grains has been linked

to numerous cases of illness and fatalities (Alameri *et al.*, 2023; Benkerroum, 2020; Meijer *et al.*, 2021), underlining the pressing need for early and effective detection methods to facilitate timely prevention and mitigation strategies. Despite the availability of various techniques such as Enzyme Linked Immunosorbent Assay (ELISA), gas chromatography (GC), and high-performance liquid chromatography (HPLC) coupled with mass spectrometry (MS), their extensive labor, cost (including solvents and instrumentation), time-consuming nature, and dependence on skilled labor limit their applicability for in-field analysis, particularly at point-of-care settings (Pérez-Fernández and de la Escosura-Muñiz, 2022; Singh and Mehta, 2020). This work was dedicated to development of an electrochemical immuno-biosensor for detection of aflatoxins in grain and cereal. The International Union of Pure and Applied Chemistry (IUPAC) define an electrochemical biosensor (Fig. 1) as an integrated, self-contained device that provides specific quantitative or semi-quantitative analytical information. This is achieved by utilizing a biological recognition element, such as an antibody, which is maintained in direct spatial contact with an electrochemical transduction element (Thévenot *et al.*, 2001). It typically consists of a biological recognition element, a transducer, a signal processing system and a read-out device.

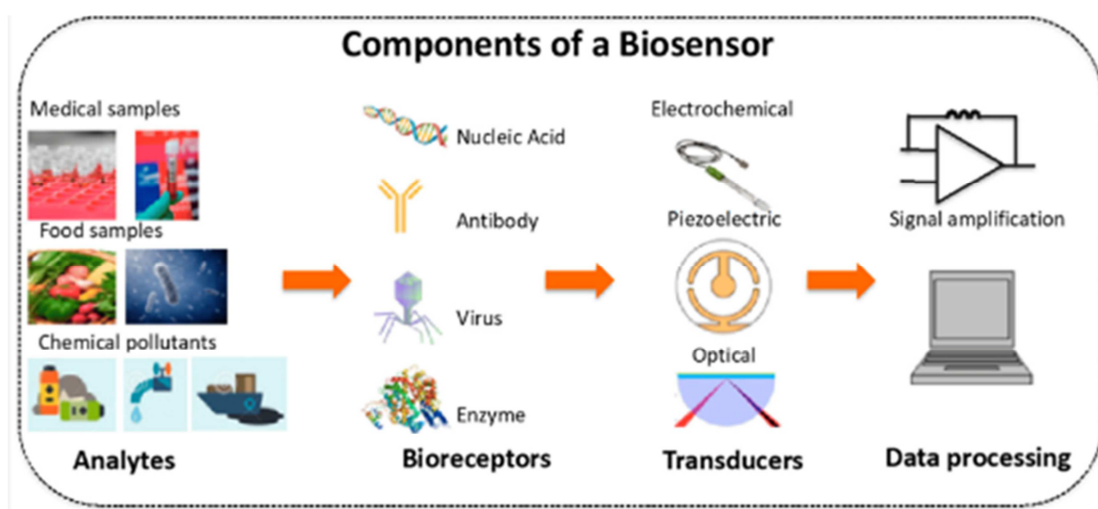


Fig. 1. Components of a biosensor (Zhou *et al.*, 2019)

The biological recognition element (bioreceptor) interacts with the target analyte, producing a measurable signal that is converted by the transducer into a quantifiable output, giving the information of existence and concentration of the target substance.

Electrochemical biosensors are widely used in various fields, including healthcare (e.g., FreeStyle Lite™ by Abbott Laboratories, for blood glucose monitoring), environmental monitoring (e.g., AquaBioTox™ by AquaBioTech, for monitoring of cyanide, ricin, or toxic metabolic products from bacteria in water bodies), and food safety (e.g., Biacore™ by Cytiva can be designed for detecting *Salmonella*, *Listeria*, *E. coli*, and other foodborne pathogens in food products), due to their remarkable selectivity, sensitivity, rapidity, robustness, and miniaturizability (field-deployability).

Moreover, they possess unique properties that combine low-cost, easy-to-use analytical procedures, requiring neither sophisticated instrumentation nor well-trained personnel to operate (Karczmarczyk *et al.* 2017; Pérez-Fernández and de la Escosura-Muñiz, 2022). Additionally, they can be seamlessly integrated into automated flow-based analysis systems (Mahadhy, 2015; Mahadhy *et al.*, 2020).

This study will address this gap through the development of a gold particles-based biosensors that can be employed in the field and be powered through Bluetooth connection to the laptop, mobile phone and related devices to help with in-field screening of aflatoxins. The laptop/mobile phone will be used for data collection hence reducing the bulkiness while enhancing portability of the detection process.

## Materials and methods

### Study area

Though the study was registered in Arusha, at the Nelson Mandela African Institute of Science and Technology (NM-AIST), all laboratory work was performed in Dar es Salaam, at the University of Dar es Salaam.

### Study site

The biosensor was developed at the University of Dar es Salaam, College of Natural and Applied Sciences, in the laboratory of the Department of Molecular Biology and Biotechnology. Maize and groundnut samples were that used in previous study by the Mycotoxins Mitigation Trial (MMT) project (Kassim *et al.*, 2022; Mollay, 2021)

### Materials

Screen-printed gold electrodes (AuSPE) (The electrodes are composed of a conventionally configuration with three-electrode, that is comprising Platinum working (0.4 mm diameter), Ag pseudo-reference and Carbon counter electrodes) in a disk-shaped were purchased from Metrohm, Switzerland, potassium ferrocyanide ( $K_4Fe(CN)_6$ ) (Merck KGaA-Germany), N-Hydroxysuccinimide (NHS) (Sigma-Aldrich-USA), N-(3-dimethylaminopropyl)-N'-ethylcarbodiimide (EDC) (Sigma-Aldrich-USA), potassium ferricyanide ( $K_3Fe(CN)_6$ ) (Merck KGaA-Germany), Aflatoxin B1 standard (Merck KGaA-Germany), 100% crystalized Bovine serum albumin (BSA) (Inqaba biotec-South Africa), monoclonal antibody anti-AFB1 were purchased from Antibodies.com (8 Station Court, Cambridge, United Kingdom), ethanolamine (Merck KGaA-Germany), Phosphate buffered saline (Inqaba biotec-South Africa). Others included analytical grade Acetic acid, sodium acetate trihydrate, acetonitrile, sulphuric acid, Methanol and Syringe filters that were procured locally. AFB1 contaminated samples of maize and groundnuts were obtained from a pool of samples that had tested positive for AFB1 by the Mycotoxins Mitigation Trial (MMT) project (Kassim *et al.*, 2022; Mollay *et al.*, 2021). The software used was the PStTrace 5 version 5.9.4515 ©2004-2023 PalmSens BV.

### Methods

#### Preparation of solutions and buffers

The Acetate buffer pH 5.6 (containing 0.1 M sodium acetate and 0.1 M acetic acid in deionized water) was prepared. Bovine Serum Albumin and antibody solution of 5 mg/mL and 5 µg/mL respectively were

prepared in acetate buffer. A solution of 5 mM  $\text{K}_4[\text{Fe}(\text{CN})_6]$ , 5 mM  $\text{K}_3[\text{Fe}(\text{CN})_6]$ , and 0.1 M KCl was then used in Differential pulse voltammetry (DPV) and Cyclic Voltammetry (CV) measurements. A blocking buffer solution was made from ethanolamine 0.1 M in deionized water. AFB1 5 mg/mL was diluted in various concentrations in order to prepare the calibration curve in acetate buffer. The solution of EDC and NHS was dissolved in distilled water.

#### Surface modification and immobilization of the antibodies

The modification of electrodes was performed with slight modifications reported by Badea *et al.* (2016). Initially, the gold electrodes were electrochemically pretreated in a 0.5 M Sulphuric acid solution by applying 10 cycles between +1.5 and -0.3 V potential versus Ag reference electrode at a scan rate of 100 mV/s (Fig. 2).

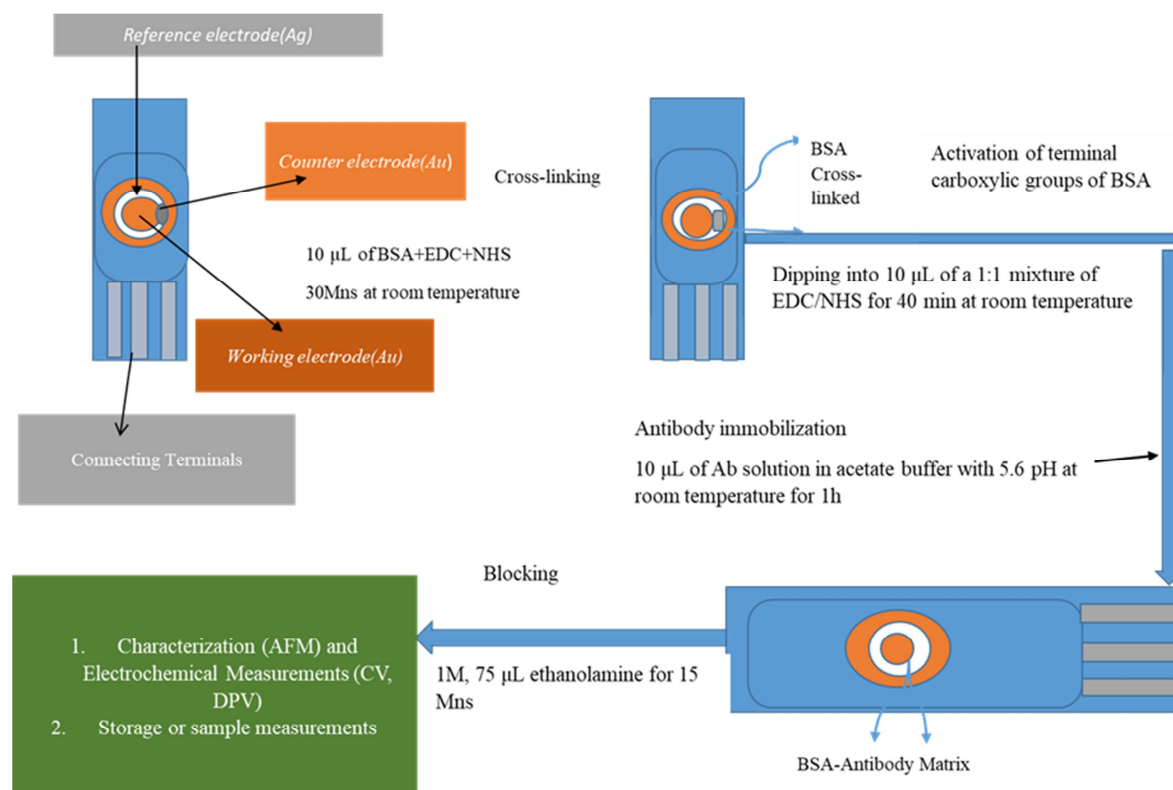


**Fig. 2.** A schematic presentation of a biosensor gold electrode modification for aflatoxin B1 detection (Re-drawn from (Karczmarczyk *et al.*, 2017))

Furthermore, it identified additional AFs until achieving a stable voltammogram, ensuring a pristine gold surface. Cleaned Au electrodes were firstly modified by cross-linked bovine serum albumin (BSA) to prevent the non-specificity in the binding of AFB1 on the Au electrode surface and allowed attachment of the antibody covalently to the activated BSA-terminal carboxylic groups. To prepare the cross-linked BSA film on the electrode surface, a mixture of 50 µL BSA (50 mg/mL), 20 µL 0.4 M EDC, and 20 µL 0.1 M NHS was incubated at 25°C for 5 minutes. Subsequently, 10

µL of this mixture was spread on the gold working electrode and left in a humid atmosphere at room temperature for 30 minutes. The electrode was then rinsed with PBS buffer and air-dried. For the immobilization of the anti-AFB1 antibody, the terminal carboxylic groups of the BSA film were activated by applying 10 µL of a 1:1 EDC/NHS mixture to the electrode surface and incubating it in a humid dark room for 40 minutes. The electrode was thoroughly rinsed with water after each step. Then, 10 µL of a 5 µg/mL anti-AFB1 antibody solution in acetate buffer (pH 5.6) was

incubated on the modified electrode for 1 hour at room temperature. The electrode was rinsed with distilled water to remove unbound antibodies. Finally, to block any pinholes, 75  $\mu\text{L}$  of 1 M ethanolamine was applied to the electrode surface and incubated for 15 minutes. Parameters for antibody immobilization, such as the concentration or amount of antibody and incubation time, were optimized for appropriate detection of AFB<sub>1</sub> in real samples, enhancing analytically good characteristics. The modified SPEs were then rinsed and stored dry at 4°C until further use.

#### *Surface characterization*

The methods used to characterize the modified SPE included the electrochemical techniques and morphological analysis.

#### *Electrochemical measurements*

Electrochemical measurements were carried out using portable electrochemical workstation (EmStat3 + Blue, PalmSens BV, Houten, The Netherlands) at room temperature. This was a small and compact, potentiostat with options to connect via Bluetooth to a mobile phone or laptop using the PStTrace 5.9 software-PalmSens, with the following parameters studied.

#### *Cyclic voltammetry*

The cyclic voltammetry (CV) study of the 10 mM Fe(CN)<sub>6</sub><sup>3-/4</sup> redox couple in 0.1 M Phosphate Buffer Saline, in the potential range of -0.2 V to +0.6 V and at a scan rate of 100 mV s<sup>-1</sup>, was employed to monitor sensor chip modifications at various steps.

#### *Differential pulse voltammetry*

The differential pulse voltammetry (DPV) study was conducted at the scan rate of 100 mV s<sup>-1</sup>, E pulse of 0.01 V, t Pulse 0.02V, E begin -0.05V and E end of 0.4V for the detection and quantification of aflatoxin in the sample. The anodic current was registered following the oxidation of aflatoxin in that applied potential range. Moreover, the registered anodic current was directly proportional to the concentration of aflatoxin in the sample.

#### *Atomic force microscope*

The surface modification was characterized using an atomic force microscope (AFM) in PBS at an ambient temperature. Firstly, the surface and topographic morphology were obtained by conducting AFM imaging (contact mode) with the tip localized into a small area on the surface of the probe. Force curves on the surface were obtained by converting the AFM imaging mode to force measurement mode with a 1 Hz ramp rate and 512 sampling points (Vidal *et al.*, 2013).

#### *Calibration curve*

The standard solutions of AFB<sub>1</sub> (ranging from 0.001 to 30 ng mL<sup>-1</sup>) were used for setting calibration curves. All the solutions were prepared in PBS. The standard curves were fitted using the "non-linear 4 parameter logistic calibration plots" as proposed by Warwick in 1996 (Moscone and Palleschi, 2006).

#### *Re-usability and selectivity*

A chosen concentration (within a linear range) was applied to the sensor multiple times with intermittent regeneration between applications until the obtained signal was less than 90% of the original (the very first one). This was done to assess how often the prepared electrode could be reused without losing its efficiency. In the selectivity study, the sensor was tested with fumonisin besides the targeted aflatoxin B<sub>1</sub> to determine if it also detected other mycotoxins.

#### *Preparation of samples*

Five-grams of known contaminated samples of groundnuts or maize were obtained from a pool of samples that had tested positive for AFB<sub>1</sub> by the Mycotoxins Mitigation Trial (MMT) project. The samples were incubated for 20 minutes in the fume hoods. The extraction of the samples was done with 25 mL of water/methanol (30:70, v/v), with the mixture being shaken for 10 minutes. It was then filtered through a 0.45  $\mu\text{m}$  syringe filter, and the extract was used for analysis.

#### *Detection of aflatoxin in real positive and negative samples*

To determine AFB<sub>1</sub> amounts, 10  $\mu\text{L}$  of AFB<sub>1</sub> standard (30 ng/mL to 0.001 ng/mL in acetate buffer, pH 5.6) or sample solution was pipetted onto the working

electrode and allowed to react for 15 minutes at ambient temperature in a humid atmosphere. The electrode was then rinsed with water before electrochemical measurements.

#### Validation of AFB1 biosensor

To validate the efficacy of our methodology, mycotoxin reference materials and internal quality control laboratory samples were selected, extracted, and analyzed following the experimental procedures outlined in the methodology section above. Subsequently, the obtained results were compared with the reference materials values. This rigorous validation process ensures the reliability and accuracy of our experimental outcomes.

## Results

#### Surface modification

Surface modification techniques were employed to functionalize the working electrode for detection of aflatoxin B<sub>1</sub>, thereby enhancing the sensitivity and specificity of the biosensor. Through electrochemical and morphological characterization, it was determined that the modified surface exhibited improved performance in detecting aflatoxin B<sub>1</sub>.

#### Electrochemical measurements

Conducting electrochemical Cyclic Voltammetry measurements utilized the traditional redox probe ferricyanide/ferrocyanide, at the formal potential of this reversible redox couple. This method serves as a practical tool to track the different phases of immunosensor development on a gold electrode (Fig. 3).

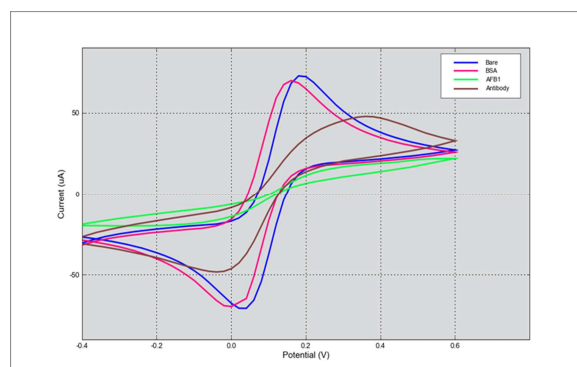


**Fig. 3.** Cyclic voltammograms

After modifying the electrodes and adding AFB<sub>1</sub> on the surface, the CV-s was performed. Fig 3 shows the CV voltammograms done in a working solution that constituted 5mM of K<sub>4</sub>Fe(CN)<sub>6</sub>, 5mM K<sub>3</sub>Fe(CN)<sub>6</sub> then mixing them with 0.1M KCl where the following parameters were set; t-equilibration (os), Ebegin (-0.6V), E-step (0.02V), E Vertex1 (0.6V), E Vertex2 (-0.6V), , scan rate (0.02V/s) and the number of scans (1) and these used for all the stages of modifications: the pretreated gold electrode, BSA/EDC/NHS/GA modified electrode, BSA/EDC/NHS/GA/anti-AFB<sub>1</sub> antibody and then BSA/EDC/NHS/GA/anti-AFB<sub>1</sub>/ 10ng/ml AFB<sub>1</sub> toxins.

#### Characterization using an atomic force microscope

The use of an AFM was for reporting and monitoring topographical changes and the variation in substrate roughness of biosensors based on various surface modifications, to examine whether there was binding, interaction, surface changes etc. (Mahadhy and Mattiasson, 2021; Sarkar, 2022) (Fig. 4).

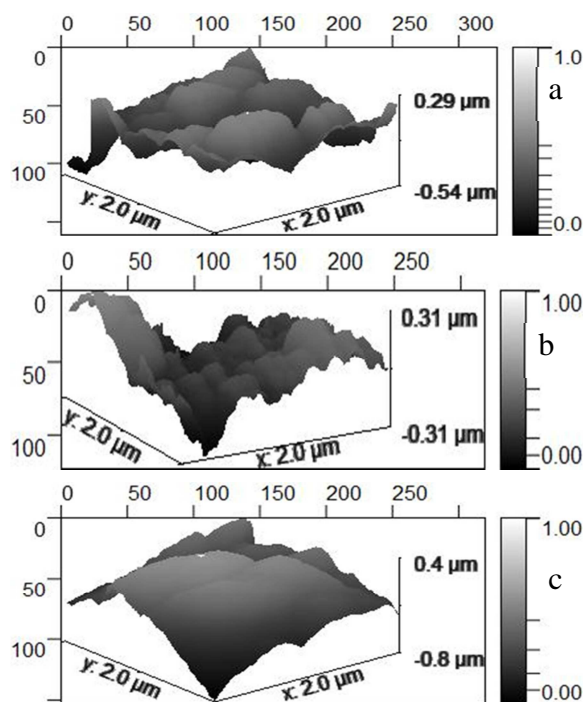


**Fig. 4.** AFM images of (a) BSA-modified SPE (b) BSA- anti-AFB<sub>1</sub>-modified SPE and (c) BSA- anti-AFB<sub>1</sub>-modified SPE bound with AFB<sub>1</sub>

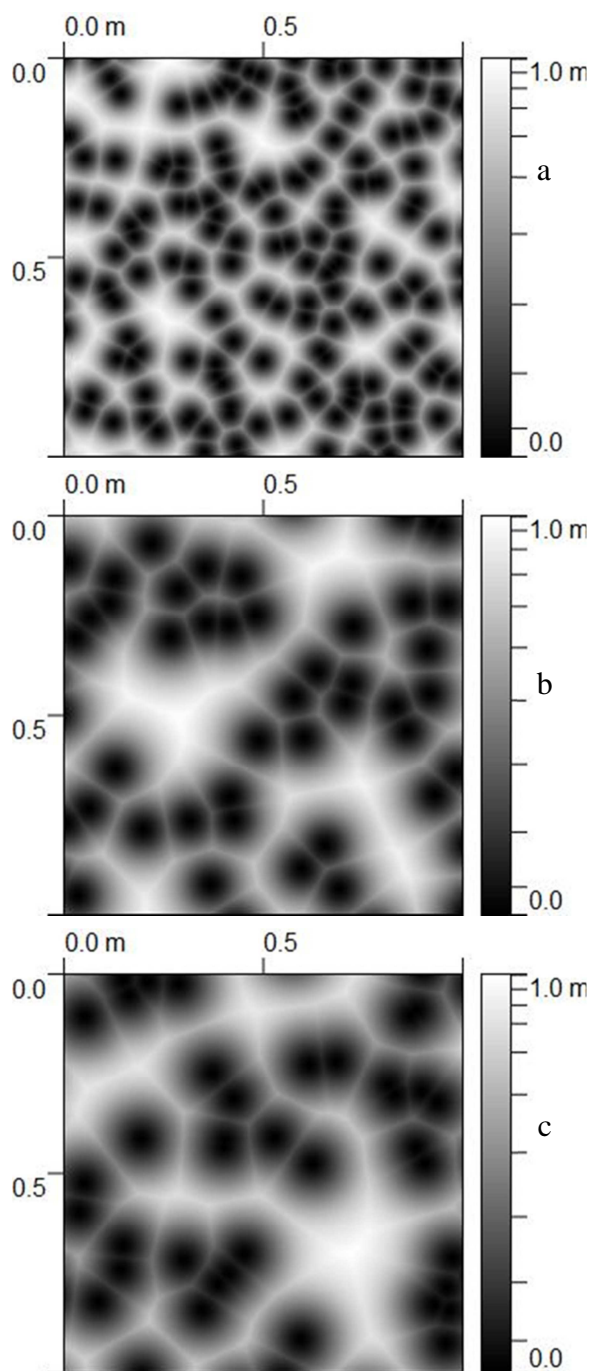


**Fig. 5.** AFM images of the lattice structures for (a) BSA-modified SPE, (b) BSA-anti-AFB1-modified SPE (c) BSA-ant-AFB1-modified SPE bound with AFB1

Based on the provided images (Fig. 5), a noticeable trend can be observed in the surface modifications of the electrodes. Image (a), depicting the modification with BSA, shows some alterations on the lattice structure of the electrode surface. Moving to image (b), where BSA and anti-AFB1 were combined for modification, the surface modifications become more apparent. Finally, in Image (c), where BSA, anti-AFB1

and AFB1 were used for modification, the lattice surface structures appear significantly obscured, indicating a successful progression of modifications.

Through AFM micrograph, the SPE surface roughness was also determined using AFM roughness parameters, i.e., maximum roughness peak height ( $R_p$ ), maximum height of the roughness ( $R_t$ ), maximum roughness valley depth ( $R_v$ ), and average maximum height of the roughness ( $R_{tm}$ ). The results are presented in Table 1 and Fig. 6 below.

**Table 1.** Peak profile analysis

Electrode	( $R_p$ ) nm	( $R_t$ ) nm	( $R_v$ ) nm	( $R_{tm}$ ) nm
BSA-modified SPE	2.23046	4.55770	2.32723	2.96582
BSA-Anti-AFB1-modified SPE	1.40974	2.50090	1.09116	1.37798
BSA-Anti-AFB1-modified SPE with AFB1	0.351171	0.728236	0.377065	0.435658

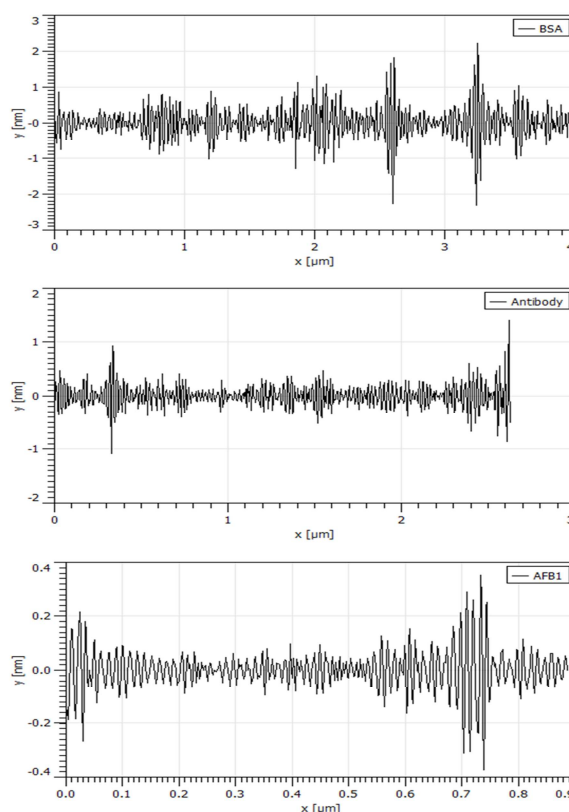


**Fig. 6.** AFM roughness graphs from results obtained in contact mode, showing roughness characteristics of: (a) BSA-modified SPE, (b) BSA-anti-AFB1-modified SPE and (c) BSA-anti-AFB1-modified SPE bound with AFB1

The variations in the Maximum roughness valley depth (Rv), and Maximum height of the roughness (Rt) values have same trend as the variations in Maximum roughness peak height (Rp) and Average maximum height of the roughness (Rtm) values for BSA cross-linked, Antibody bound and AFB1 bound electrodes.

#### Establishment of calibration curve (Limit of detection, limit of blank, and linearity range)

To determine the LoB, and LoD, the blank, and the standards (Fig. 7) were used to establish the limits as suggested by (Armbruster and Pry, 2008) using the formulae

$$\text{LoB} = \text{mean blank} + 1.645(\text{SD blank}) (\mu\text{A})$$

$$\text{LoD} = \text{LoB} + 1.645(\text{SD low concentration of standard}) (\mu\text{A})$$

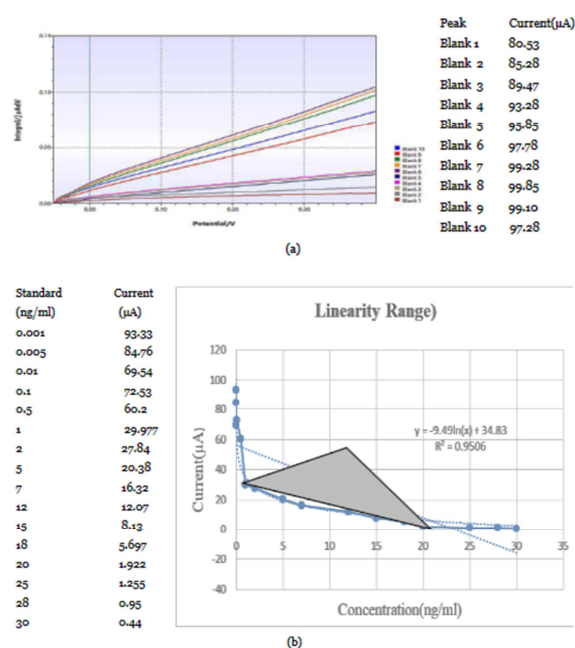


**Fig. 7.** (a) Graph showing current peaks obtained from a blank sample (0.0 ng/ml) and standard samples of different concentrations (0.001 to 30 ng/ml). (b) Calibration curve established from the data in graph (a) above, indicating the Limits of Blank (LoB) and Limits of Detection (LoD), as well as the linearity range

In this research, we ascertained the upper limit of the apparent analyte concentration in replicates of a blank sample (LoB), to be 1.67 ng/ml.

Simultaneously, we established the Limit of Detection (LoD) at 2.058 ng/ml, representing the minimal analyte concentration reliably distinguishable from the LoB and conducive to feasible detection.

#### Study on re-usability

To assess the frequency of sensor chip reusability without compromising efficiency, a 10 ng/ml concentration of the AFB1 standards was applied to the sensor chip ten times, with intermittent regeneration between applications, until the obtained signal was less than 90% of the original signal (Fig. 8). The regenerating solution consisted of a mixture of 5 mM NaOH and 1% SDS in a 1:1 ratio. To achieve this, we applied 10 μL of the solution and incubated the electrode for 5 minutes at room temperature. During this electrochemical cleaning process, we used differential pulse voltammetry to observe changes in peaks between washes and compared them to the voltamograms obtained with 15 ng/mL AFB1. It was found that repetitive measurements are possible up to five times while maintaining reproducibility. This method is believed to enable accurate monitoring of biological effects, long-term and reuse of sensor chips, particularly at a low cost.

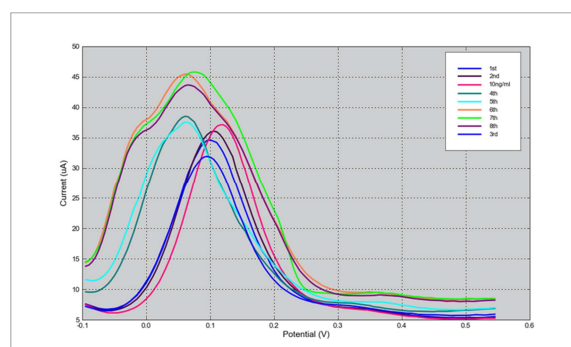


**Fig. 8.** Reusability DPV curves

After the 5th wash, there were noticeable and inconsistent peak shifts, although the peaks in the first 5 washes were well-defined and nearly identical, the same pattern of regeneration was also observed by Lee *et al.* 2023. The irregularities observed from the 6th to 8th washes could potentially be attributed to the blocking or scratching of the working electrode surface due to regeneration cycles. For the five regeneration there more than 90% efficiency (Fig. 9),



and a suitable solution has been identified to ensure their proper reusability.

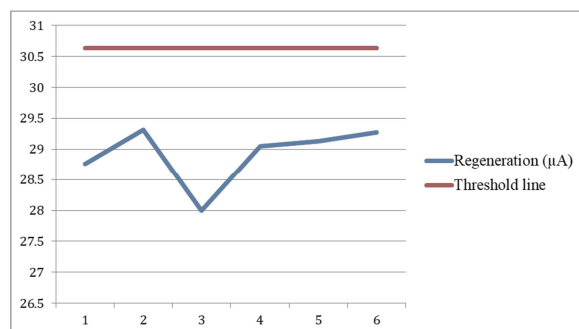


**Fig. 9.** A graph depicting the data point pattern at various electrode residual capacity percentages, ranging from 100% to >90%, along with a threshold line

*Study on the selectivity*

In investigating the selectivity of the biosensor, we exposed it to samples containing AFB1 and fumonisin, each at a concentration of 4ng/ml (Fig. 10). The depicted figure illustrates the distinctions between AFB1 and fumonism, underscoring the biosensor's capability to selectively differentiate between various types of mycotoxins. This observation highlights the biosensor's effectiveness in discerning specific mycotoxin types, a crucial feature in its analytical performance.

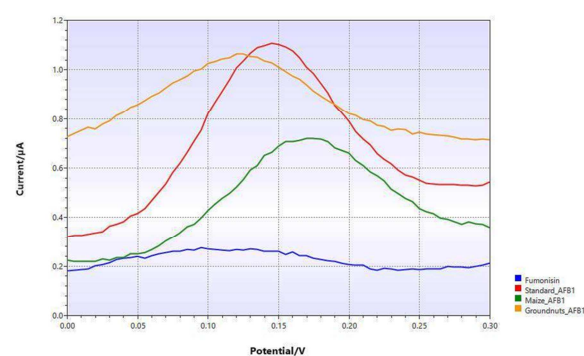


**Fig. 10.** The response of the biosensor on fumonisin and AFB1 in a standard, maize sample and groundnuts samples

*Validation and detection of AFB1 in real samples*

To assess the feasibility of this approach, we conducted an analysis to validate the presence of aflatoxin B1

(AFB1) in real-world samples where the samples were prepared as explained in the method section. These samples encompassed spiked contaminated maize flour, mycotoxin reference materials sourced from Neogen-USA, as well as internally maintained quality control maize and peanut samples. The findings of the study, detailed in Table 2 and 3, reveal recovery rates ranging from 90% to 105%.

**Table 2.** Effect of biological matrix

Sample	Known Concentration (ng/ml)	Detected concentration (ng/ml)	Recovery rate (%)
Reference material	4	4.179	104
Spiked corn	4	3.6	90
Internal QC-maize	4	4.2	105
Internal QC-groundnuts	4.0	4.18	104

**Table 3.** Validation study

Sample	Biosensor (ng/ml)	ELISA (ng/ml)
Reference material	4.179	4
Spiked corn	3.6	4
Internal QC-maize	4.2	4
Internal QC-groundnuts	4.18	4
Correlation		0.92
P-Value		0.04

Both ELISA and biosensor experiments were carried out maize, groundnut samples and standards. The correlation between developed biosensor and standard ELISA technique has shown error-free results of 92% in the tested samples and this correlation is significant (Table 3).

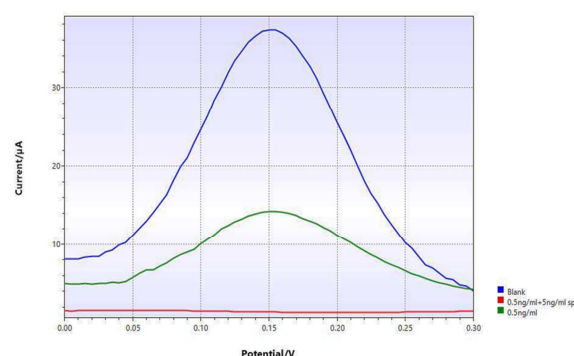


**Fig. 11.** Detection of AFB1 using the developed biosensor

From the Fig. 11 above, the blue line shows a peak current for blank sample; green is for maize sample with 0.5 ng/ml, while the red line shows the biosensor response to the 0.5 ng/ml maize sample spiked with 5 ng/ml standard. When 0.5 ng/ml AFB1 maize sample was spiked with the 5 ng/ml standard, the peak current decreased (green curve to red curve). This outcome evidently establishes the AFB1 sensing capability of the present method in grain samples. A designed prototype of the biosensor is given below (Fig. 12).

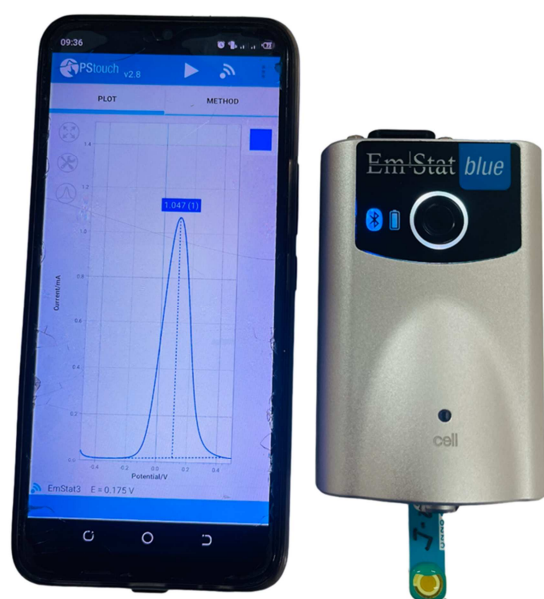


**Fig. 12.** Designed prototype of the biosensor where Mobile phone (left), a potable potentiostat (right) and an electrode attached to the potentiostat are all connected/communicate through Bluetooth

## Discussion

### *Electrochemical measurements*

With modifications, there was change in CV properties with bare and BSA cross-linked electrodes having higher oxidation and reduction current, antibody bound electrode low and AFB1 bound electrodes had the lowest oxidation-reduction current. The decrease in redox peak currents after modifications (bare, BSA cross-linked, anti-AFB1 bound and AFB1 attached) reflects the passivation of the electrode surface, because the formed layers hampers the electron transfer between electrode surface and redox species. Following immobilization

of the capture probe onto the surface with AFB1, the redox peak currents were further decreased. This was similar to the studies performed by Mahadhy *et al.*, 2014a; Mahadhy *et al.*, 2014b; Mahadhy *et al.*, 2021; ; Moon *et al.*, 2018.

### *Characterization using an atomic force microscope*

Considering both the cyclic voltammetry (CV) and atomic force microscopy (AFM) images, it is evident that the surface of the electrodes underwent successful modifications. The increasing obscuration of the surface lattice structures with each progressive modification provides visual confirmation of the changes made to the electrode surfaces. The images were analyzed using Gwyddion 2.65, free and open-source software for scanning probe microscopy data visualization and analysis, which was released in 2021. The analysis showed the decrease in roughness was modified for instance the  $R_t$  values decreased from 4.56 for BSA cross-linked sensor chip to 2.5 and 0.73 nm for antibody bound and AFB1 bound electrode respectively. Peak to valley height ( $R_{pv}$ ) is considered a crucial parameter as it effectively describes the overall roughness of a surface. It is defined as the vertical distance from the highest peak to the lowest valley across the entire evaluation length of the profile. Results from topographical images and peak height profile analysis demonstrate the presence of self-organization following modifications, resulting in a highly ordered and smooth surface (Mahadhy and Mattiasson, 2021).

### *Calibration curve, selectivity and validation*

This study established that the limit of blank sample (LoB), to be 1.67 ng/ml while the Limit of Detection (LoD) being 2.058 ng/ml, with this limit of detection makes it a good candidate for field deployment and rapid detection of AFB1. To determine the linearity range above, the concentration-response relationship of the assay was evaluated using the provided data. From the table, the current response decreases as the concentration of the analyte increases, indicating a linear relationship between concentration and response within the tested range spanning from 0.001 ng/ml to 30ng/ml. This range encompasses the

concentrations used for establishing the Limit of Detection (LoD) and ensures that the assay response remains linear within this concentration range. These observations give the concentration interval over which the assay provides a consistent and predictable response to changes in analyte concentration. This biosensor prototype indicated that there was weak response on samples contaminated with fumonisin (4ng/ml) compared to the AFB<sub>1</sub> standard (4ng/ml), AFB<sub>1</sub> containing maize flour (4ng/ml) and AFB<sub>1</sub> containing groundnuts at 4ng/ml. This result suggests that the present method can detect AFB<sub>1</sub> selectively without a cross reaction of fumonisin. This suggests that the proposed sensor holds promise for the quantitative determination of AFB<sub>1</sub> in agricultural commodity samples. These results were similar to (Hu *et al.*, 2021) study. Through the use of this biosensor, the study achieved a low limit of blank sample (LoB) (1.67 ng/ml) and a low Limit of Detection (LoD) (2.058 ng/ml) with these values being below the set limits of total aflatoxins in food stuffs for most of the regulatory authorities in different organizations globally, like India (30 µg/kg), Singapore (5 µg/kg), European Union (4 µg/kg), China (20 µg/kg) USA and Canada (15 µg/kg) (Mamo *et al.* 2021) and Tanzania-AFB<sub>1</sub> (10 µg/kg) (Seetha *et al.* 2017) and AFB<sub>1</sub> recovered from spiked food samples was successfully detected. In addition, the result showed high selectivity against fumonisin, paving a way for other studies to assess other mycotoxins cross reactivity.

### Conclusion

This study developed a sensitive, specific and affordable biosensor for field detection of Aflatoxin B<sub>1</sub> in grains. With the detection limit, design and flexibility that this biosensor can attain, it can be used for quantitatively measuring the Aflatoxin B<sub>1</sub> contents in grains. This biosensor has shown improved and shortened processing time, portability, low detection limits, simplicity, and thus could be field deployable. In addition, the result showed high selectivity against fumonisin, paving a way for other studies to assess other mycotoxins cross reactivity. This study recommends further investigations especially on

exploring different materials, selectivity of the biosensor against different types of mycotoxins in wide range of matrices to affirm its selectivity.

### Acknowledgements

The authors extend gratitude to the Mycotoxin Mitigation Trial project at the Nelson Mandela African Institution of Science and Technology for supplying reference samples and standards. Special thanks are due to collaborators from the Department of Food Biotechnology and Nutritional Sciences, School of Life Sciences and Bio-Engineering (LiSBE) at the Nelson Mandela African Institution of Science and Technology (NM-AIST), Arusha, and the Department of Molecular Biology and Biotechnology at the University of Dar es Salaam, Tanzania, for their indispensable contributions to this study.

### References

- Alameri MM, Kong AS-Y, Aljaafari MN, Ali HA, Eid K, Sallagi MA, Cheng W-H, Abushelaibi A, Lim S-HE, Loh J-Y.** 2023. Aflatoxin contamination: An overview on health issues, detection, and management strategies. *Toxins* **15**(4).
- Armbruster DA, Pry T.** 2008. Limit of blank, limit of detection and limit of quantitation. *The Clinical Biochemist Reviews* **29 Suppl 1(Suppl 1)**, S49-52.
- Benkerroum N.** 2020. Chronic and acute toxicities of aflatoxins: Mechanisms of action. *International Journal of Environmental Research and Public Health* **17**(2).
- Chen J, Wen J, Tang Y, Shi J, Mu G, Yan R, Cai J, Long M.** 2021. Research progress on fumonisin B<sub>1</sub> contamination and toxicity: A review. *Molecules* (Basel, Switzerland) **26**(17).  
<http://dx.doi.org/10.1016/j.bios.2013.05.008>.
- Hu D, Xiao S, Guo Q, Yue R, Geng D, Ji D.** 2021. Luminescence method for detection of aflatoxin B<sub>1</sub> using ATP-releasing nucleotides. *RCS Advances* **11**(24027), 24027–31.

- Kamle M, Mahato DK, Devi S, Lee KE, Kang SG, Kumar P.** 2019. Fumonisin: Impact on agriculture, food, and human health and their management strategies. *Toxins* **11(6)**.
- Karczmarczyk A, Bäumner AJ, Feller K-H.** 2017. Development of biosensors for mycotoxins detection in food and beverages. Fakultät für Chemie und Pharmazie Ph.D., XXII, 135. [https://epub.uni-regensburg.de/36587/1/A.Karczmarczyk\\_thesis.pdf](https://epub.uni-regensburg.de/36587/1/A.Karczmarczyk_thesis.pdf)
- Kassim N, Makule E, Smith LE, Nelson R.** 2022. Ethical considerations in the design and conduct of a cluster-randomized mycotoxin mitigation trial in Tanzania.
- Kassim N, Ngure F, Smith L, Turner PC, Stoltzfus R, Makule E, Makori N, Phillips E.** 2023. Provision of low-aflatoxin local complementary porridge flour reduced urinary aflatoxin biomarker in children aged 6–18 months in rural Tanzania. *Maternal & Child Nutrition* **19(e13499)**, 1–9.
- Lee J, Suh HN, Park HB, Park YM, Kim HJ, Kim S.** 2023. Regenerative strategy of gold electrodes for long-term reuse of electrochemical biosensors. *ACS Omega* **8**, 1389–1400.
- Magoha H, Kimanya M, De Meulenaer B, Roberfroid D, Lachat C, Kolsteren P.** 2014. Risk of dietary exposure to aflatoxins and fumonisins in infants less than 6 months of age in Rombo, Northern Tanzania. *Maternal & Child Nutrition IARC* **2002**, 1–12.
- Mahadhy A, Mamo G, Ståhl-Wernersson E, Mattiasson B, Hedström M.** 2014. PCR-free ultrasensitive capacitive biosensor for selective detection and quantification of Enterobacteriaceae DNA. *Analytical & Bioanalytical Techniques* **5(5)**.
- Mahadhy A, Mattiasson B.** 2021. Evaluation of polytyramine film and 6-mercaptohexanol self-assembled monolayers as the immobilization layers for a capacitive DNA sensor chip: A comparison. *Sensors (Switzerland)* **21(8149)**.
- Mahadhy A, Ståhl-wernersson E, Mattiasson B, Hedström M.** 2014. Use of a capacitive affinity biosensor for sensitive and selective detection and quantification of DNA—a model study. *Biotechnology Reports* **3**, 42–48.
- Mahadhy A, Ståhl-Wernersson E, Mattiasson B, Hedström, M.** 2020. Rapid detection of Meca gene of methicillin-resistant *Staphylococcus aureus* by a novel, label-free real-time capacitive biosensor. *Biotechnology Reports* **28**.
- Mahadhy A.** 2015. Development of an ultrasensitive capacitive DNA-sensor: A promising tool towards microbial diagnostics.
- Mamo FT, Abate BA, Zheng Y, Nie C, He M, Liu Y.** 2021. Distribution of *Aspergillus* fungi and recent aflatoxin reports, health risks, and advances in developments of biological mitigation strategies in China. *Toxins* **13(10)**.
- Meijer N, Kleter G, de Nijs M, Rau ML, Derkx R, van der Fels-Klerx HJ.** 2021. The aflatoxin situation in Africa: Systematic literature review. *Wiley (February)*, 2286–2304.
- Mollay C, Kassim N, Stoltzfus R, Kimanya M.** 2020. Childhood dietary exposure of aflatoxins and fumonisins in Tanzania: A review. *Cogent Food & Agriculture* **6(1)**, 1859047. <https://doi.org/10.1080/23311932.2020.1859047>.
- Mollay C, Kassim N, Stoltzfus R, Kimanya M.** 2021. Complementary feeding in Kongwa, Tanzania: Findings to inform a mycotoxin mitigation trial study site. *Maternal & Child Nutrition* **17(e13188)**, 1–10.
- Mollay C, Kimanya M, Kassim N, Stoltzfus R.** 2022. Main complementary food ingredients contributing to aflatoxin exposure to infants and young children in Kongwa, Tanzania. *Food Control* **135**, 108709. <https://www.sciencedirect.com/science/article/pii/S0956713521008471>.

- Mollay C.** 2021. Complementary feeding in Kongwa, Tanzania: Findings to inform a mycotoxin mitigation trial. John Wiley & Sons Ltd.
- Moon J, Byun J, Kim H, Lim EK, Jeong J, Jung J, Kang T.** 2018. On-site detection of aflatoxin B1 in grains by a palm-sized surface plasmon resonance sensor. *Sensors (Switzerland)* **18(2)**.
- Mosccone D, Palleschi G.** 2006. Detection of aflatoxin B1 in barley: Comparative study of immunosensor and HPLC.
- Pérez-Fernández B, de la Escosura-Muñiz A.** 2022. Electrochemical biosensors based on nanomaterials for aflatoxins detection: A review (2015–2021). *Analytica Chimica Acta (xxxx)*.
- Phillips E, Ngure F, Smith LE, Makule E, Turner PC, Nelson R, Kimanya M, Stoltzfus R, Kassim N.** 2020. Protocol for the trial to establish a causal linkage between mycotoxin exposure and child stunting: A cluster randomized trial. *BMC Public Health* **20(1)**, 598.  
<https://doi.org/10.1186/s12889-020-08694-6>.
- Pickova D, Ostry V, Malir J, Toman J, Malir F.** 2020. A review on mycotoxins and microfungi in spices in the light of the last five years. *Toxins* **12(12)**, 1–33.
- Sarkar A.** 2022. Biosensing, characterization of biosensors, and improved drug delivery approaches using atomic force microscopy: A review. *Frontiers in Nanotechnology* **3(January)**, 1–19.
- Seetha A, Munthali W, Msere HW, Swai E, Muzanila Y, Sichone E, Tsusaka TW, Rathore A, Okori P.** 2017. Occurrence of aflatoxins and its management in diverse cropping systems of central Tanzania. *Mycotoxin Res.* **33(4)**, 323–331.  
DOI: 10.1007/s12550-017-0286-x.
- Singh J, Mehta A.** 2020. Rapid and sensitive detection of mycotoxins by advanced and emerging analytical methods: A review. *Food Science and Nutrition* **8(5)**, 2183–2204.
- Smith GW.** 2007. Chapter 78 - Fumonisin. In *Veterinary Toxicology*, ed. Ramesh C Gupta. Academic Press, 983–96.  
<https://www.sciencedirect.com/science/article/pii/B9780123704672501759>.
- Smith GW.** 2018. Chapter 71 - Fumonisin. In *Veterinary Toxicology (Third Edition)*, ed. Ramesh C Gupta. Academic Press, 1003–18.  
<https://www.sciencedirect.com/science/article/pii/B9780128114100000714>.
- Steyn PS.** 2023. Chapter 12 - Mycotoxins in cereals. In *ICC Handbook of 21st Century Cereal Science and Technology*, eds. Peter R Shewry, Hamit Koksel, John R N Taylor. Academic Press, 111–19.  
<https://www.sciencedirect.com/science/article/pii/B9780323952958000368>.
- Thévenot DR, Toth K, Durst RA, Wilson GS.** 2001. Electrochemical biosensors: Recommended definitions and classification. *Biosensors & Bioelectronics* **16**, 121–31.
- Vidal JC, Bonel L, Ezquerro A, Hernández S, Bertolín JR, Cubel C, Castillo JR.** 2013. Electrochemical affinity biosensors for detection of mycotoxins: A review. *Biosensors and Bioelectronics* **49**, 146–158.
- Zhou Y, Fang Y, Ramasamy RP.** 2019. Non-covalent functionalization of carbon nanotubes for electrochemical biosensor development. *Sensors (Switzerland)* **19(2)**.